



# Computational non-smooth fracture dynamics in nonlinear and heterogeneous materials. Application to fracture of hydrided Zircaloy

Frédéric Perales, Yann Monerie, Frédéric Dubois, Laurent Stainier

## ► To cite this version:

Frédéric Perales, Yann Monerie, Frédéric Dubois, Laurent Stainier. Computational non-smooth fracture dynamics in nonlinear and heterogeneous materials. Application to fracture of hydrided Zircaloy. 18th International Conference on Structural Mechanics in Reactor Technology (SMiRT 18), Aug 2005, Pékin, China. hal-00580799

**HAL Id: hal-00580799**

**<https://hal.science/hal-00580799>**

Submitted on 30 Nov 2016

**HAL** is a multi-disciplinary open access archive for the deposit and dissemination of scientific research documents, whether they are published or not. The documents may come from teaching and research institutions in France or abroad, or from public or private research centers.

L'archive ouverte pluridisciplinaire **HAL**, est destinée au dépôt et à la diffusion de documents scientifiques de niveau recherche, publiés ou non, émanant des établissements d'enseignement et de recherche français ou étrangers, des laboratoires publics ou privés.

# COMPUTATIONAL NON-SMOOTH FRACTURE DYNAMICS IN NONLINEAR AND HETEROGENEOUS MATERIALS. APPLICATION TO FRACTURE OF HYDRIDED ZIRCALOY

**F. Perales\***

*Institut de Radioprotection et de Sûreté  
Nucléaire  
IRSN/DPAM/SEMCA/LEC  
Bat 702 - CE Cadarache - BP3  
13115 St Paul-Lez-Durance cedex, France  
Phone: +33 (0)4 42 25 30 54, Fax: +33 (0)4  
42 25 61 43  
E-mail: frederic.perales@irsn.fr*

**Y. Monerie**

*Institut de Radioprotection et de Sûreté  
Nucléaire  
IRSN/DPAM/SEMCA/LEC  
Bat 702 - CE Cadarache - BP3  
13115 St Paul-Lez-Durance cedex, France*

**F. Dubois**

*Laboratoire de Mécanique et Génie Civil  
LMGC/UMR CNRS 5508, University  
Montpellier II,  
CC048, Place Eugene Bataillon  
34095 Montpellier cedex 5, France*

**L. Stainier**

*Département Aéronautique, Mécanique et  
Matériaux  
LTAS-MCT, University of Liège  
1 chemin des chevreuils  
4000 Liège, Belgium*

## ABSTRACT

This paper presents a new computational method and the associated software dedicated to the study of the dynamic fracture of nonlinear and heterogeneous materials. This method is based on the concept of Frictional Cohesive Zone Model in the framework of Non-Smooth Contact Dynamics. The associated numerical platform, composed of three object-oriented libraries, allows to simulate, in three dimensional finite deformations, the dynamic fracture of both multiphase and functionally graded materials from crack initiation to post-fracture behavior. The ability of this software, developed by the French 'Institut de Radioprotection et de Sûreté Nucléaire' (IRSN) in the frame of its research program on nuclear fuel safety, is illustrated on the fracture of hydrided Zircaloy-4, constituting nuclear cladding tubes at high burnup, during a reactivity initiated accident (RIA). The macroscopic behavior of this heterogeneous material is deduced as an averaged energy release rate depending on the volume fraction of hydride phase.

**Keywords :** Fissuration, non smooth dynamics, cohesive zone model, numerical simulation, hydrided Zircaloy-4

## 1 INTRODUCTION

Zirconium alloys like Zircaloy-4 are metals used as the cladding material of nuclear fuel rods in Pressurized Water Reactor (PWR). During nuclear reactor operation, bulk microstructure of these metals evolves because of

hydrogen which precipitates as zirconium hydrides. So, the microstructure of fuel cladding tubes appears as a bimaterial constituted of hydride embedded in a metal matrix. To analyse the effects of this microstructure heterogeneity on material behavior, we use a computational micromechanical approach.

The micromechanical approach considered in this work is based on the concept of Frictional Cohesive Zone Model (FCZM) which represents the mechanical processes in the fracture process zone in front of a crack tip. The FCZM allows simulation of crack initiation (without any *ad hoc* criteria), crack propagation (crack path is not known in advance) and non-smooth surfacic behavior such as unilateral contact and friction, in heterogeneous materials at several scales. The mechanical separation is described by a constitutive equation relating applied stress on the crack lips to the displacement jump between each element of a finite element modeling. Each mesh is, thus, considered as an independant body connected to another by non-linear and non-smooth relations.

Since velocity can become discontinuous during dynamic fracture, the Non-Smooth Contact Dynamic (NSCD) approach is used. This approach, initiated by Moreau (1988) and Jean (1999), consists in solving non-smooth equations of frictional contact without any regularization nor penalization.

The numerical platform, developed by the French 'Institut de Radioprotection et de Sûreté Nucléaire' (IRSN) in the frame of its research program on nuclear fuel safety, is composed of three libraries : a Fortran90 library dedicated to surfacic behaviors related to FCZM in the NSCD approach (LMGC90), a C++ library dedicated to Finite Element modeling (PELICANS) and a C++ library dedicated to bulk constitutive models (MATLIB).

The ability of the numerical platform is illustrated on the dynamic fracture of hydrided Zircaloy-4 under transient loading. A study is performed to determine the macroscopic behavior of hydrided Zircaloy-4 as function of hydrogen content.

## 2 FRICTIONAL COHESIVE ZONE MODEL (FCZM)

The FCZM considered here is a model coupling cohesion with unilateral contact and Coulomb friction inspired by the cohesive law of Raous et al. (1999); Raous and Monerie (2002). A cohesive reaction, denoted  $R^{coh}$ , is added to the unilateral contact problem (Eq. 1) and the Coulomb friction problem (Eq. 2).

$$0 \leq (R_N + R_N^{coh}) \perp u_N \geq 0 \quad (1)$$

$$\begin{cases} \|R_T + R_T^{coh}\| < \mu |R_N + R_N^{coh}| \Rightarrow \dot{u}_T = 0 \\ \|R_T + R_T^{coh}\| = \mu |R_N + R_N^{coh}| \Rightarrow \exists \lambda \geq 0 \text{ such as } \dot{u}_T = -\lambda(R_T + R_T^{coh}) \end{cases} \quad (2)$$

Subscripts  $N$  and  $T$  respectively denote the normal and tangential component of the total force ( $R = R_N n + R_T$ ), the cohesive force ( $R^{coh} = R_N^{coh} n + R_T$ ) and the displacement jump ( $[u] = u_N n + u_T$ ),  $n$  is the unit normal vector of the cohesive zone. The friction coefficient is denoted  $\mu$ .

In this study, in order to particularize the FCZM, we use the cohesive force described by Eq. 3, initially introduced by Fremond (1987), based on a surfacic variable  $\beta$  (Eq. 4) ( $\beta = 1$  : the cohesion is complete,  $0 < \beta < 1$  : the cohesion is partially broken and  $\beta = 0$  : there is no cohesion).

$$R^{coh} = \begin{cases} K(\beta) \cdot [u] & \text{if } \beta > 0 \text{ or } u_N = 0 \\ K(\beta) \cdot [u] - p \cdot n & \text{otherwise} \end{cases} \quad (3)$$

$$\beta = \min(g(\|[u]\|), g(\|[u_{\max}]\|)) \quad (4)$$

where  $u_{\max}$  is the maximum value reached by  $u$ ,  $K(\beta)$  is a matrix describing the progressive surfacic softening behavior during crack propagation,  $p$  denotes internal post-fracture pressure (MPa) and  $g$  is a decreasing function of  $\|[u]\|$ .

We use a variant of the surfacic damage law defined by Michel et al. (1994) :

$$K(\beta) = \beta \left( C_N n \otimes n + C_T \frac{u_T \otimes u_T}{\|u_T\|^2} \right)$$

$$g(x) = \begin{cases} \beta_0 & \text{if } x \leq \delta_0 \\ 0 & \text{if } x \geq \delta_c \\ \frac{\beta_0(\delta_c - x)}{\delta_c - 2\delta_0 + x} & \text{otherwise} \end{cases}$$

where  $\delta_0 = \sqrt{\frac{w}{(9 - 4\ln 4)} \left( \frac{1}{C_N} + \frac{1}{C_T} \right)}$ ,  $\delta_c = 3\delta_0$ ,  $C_N$  and  $C_T$  are the initial normal and tangent stiffness to the interface if cohesion is complete (MPa/m),  $0 \leq \beta_0 \leq 1$  is a initial surface damage and  $w$  is a reference fracture energy (J/m<sup>2</sup>).

In a 2D case, Figure 1 shows the normal behavior (with  $u_T = 0$ ) and the tangential behavior (with  $R_N$  constant).

PSfrag replacements

PSfrag replacements

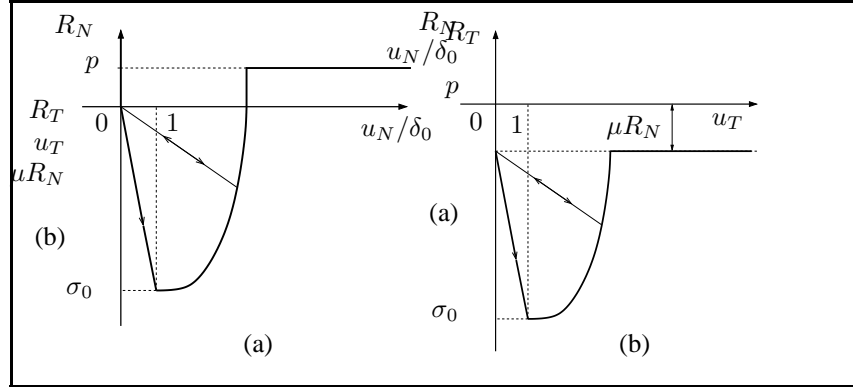


Figure 1: 2D cohesive law : (a) normal behavior ( $u_T = 0$ ) (b) tangent behavior ( $R_N$  constant and  $u_N = 0$ ).

When decohesion vanishes ( $\beta = 0$  in this model), we obtain the classical Signorini problem for the normal behavior and the Coulomb friction problem for the tangential behavior.

### 3 NON-SMOOTH CONTACT DYNAMICS (NSCD)

#### 3.1 The equation of dynamics

The dynamic problem is composed by the Eqs. 1-4 and the discrete dynamic equation :

$$M\ddot{q} = F(q, \dot{q}, t) + r \quad (5)$$

where  $q$ ,  $\dot{q}$  and  $\ddot{q}$  respectively are discrete displacement, velocity and acceleration,  $F(q, \dot{q}, t)$  represents internal and external forces and  $r$  is representative of local reaction forces.

Since shocks are expected, the velocity  $\dot{q}$  can be a step function and the acceleration  $\ddot{q}$ , then, cannot be defined. In this way, Eq. 5 is solved using NSCD approach (Jean, 1999) within the functional framework proposed by Moreau (1988). Particularly, the derivative in the dynamic equation are to be understood in the sense of distributions.

#### 3.2 Time discretization

Denoting by a subscript  $i$  quantities at a time  $t_i$  and by  $i + 1$  quantities at time  $t_{i+1}$ , the numerical method ( $\theta$ -method) can be written over the time interval  $]t_i, t_{i+1}]$  as :

$$\begin{cases} M_{i+1}(\dot{q}_{i+1} - \dot{q}_i) = h[(1 - \theta)F_i + \theta F_{i+1}] + hr_{i+1} \\ q_{i+1} = q_i + h[(1 - \theta)\dot{q}_i + \theta\dot{q}_{i+1}] \end{cases} \quad (6)$$

where  $hr_{i+1}$  is the mean impulse value. The unknowns of the problem are the approximations of the velocity  $\dot{q}_{i+1}$  and the impulse  $hr_{i+1}$ .

A Newton-Raphson algorithm is used to solve the non-linear set of discretized equations (6) :

$$\begin{cases} \dot{q}_{i+1}^{k+1} = \dot{q}_{i+1}^k + \Delta \dot{q}_{\text{free}} + hw^k r_{i+1}^{k+1} \\ \Delta \dot{q}_{\text{free}} = w_{i+1}^k \{-M_{i+1}^k(\dot{q}_{i+1}^k - \dot{q}_i) + h[(1-\theta)F_i + \theta F_{i+1}^k] + hr_{i+1}^k\} \end{cases} \quad (7)$$

where  $k$  stands for iterations,  $w_{i+1}^k$  is the inverse of the iteration matrix.

### 3.3 Non-Smooth Contact Dynamics and Frictional Cohesive Zone Model

Using linear mappings between global values (velocity  $\dot{q}$  and impulse  $hr$ ) and their relative values ( $\dot{u}$  and  $hR$ ), and a change of variable introduced by Monerie and Acary (2001), the three dimensional system to solve for each contact  $\alpha$  writes (Jean et al., 2001) :

$$\begin{cases} U^\alpha - U_{locfree}^\alpha + W^{\alpha\alpha}h(R - R^{coh})^\alpha = 0 \\ R_N^\alpha - \text{proj}_{\mathbb{R}^-}(R_N^\alpha + \rho U_N^\alpha) = 0 \\ R_T^\alpha - \text{proj}_{D(\mu|R_N^\alpha|)}(R_T^\alpha + \rho U_T^\alpha) = 0 \end{cases} \quad (8)$$

where  $\rho > 0$  and  $D(\mu|R_N^\alpha|)$  is the section of Coulomb's cone for contact  $\alpha$  i.e. the disc with center 0 and radius  $\mu|R_N^\alpha|$  and  $U_{locfree}^\alpha$  is the velocity at the contact  $\alpha$  without any reaction coming from the FCZM.

The system (8) may be written as a mapping  $\phi$  :

$$\phi(U^\alpha, R^\alpha) = 0 \quad (9)$$

and solved using the generalized Newton method of Alart and Curnier (1988).

## 4 NUMERICAL PLATFORM

The numerical platform is composed of three libraries with Object Oriented Programming (OOP) concepts. This design increases software flexibility (reusability makes the existing code easier to modify and extend its functionality and capabilities). The three libraries are coupled with an encapsulated design and each module has a clear meaning from a mechanical point of view :

- *LMGC90* is a Fortran90 library dedicated to surfacic behaviors related to FCZM in the NSCD approach. It is developed at the Laboratory of Mechanics and Civil Engineering by Dubois and Jean (2003).
- *PELICANS* is a C++ Finite Element library developed by the French 'Institut de Radioprotection et de Sûreté Nucléaire' (IRSN) (Piar et al., 2003).
- *MATLIB* is a C++ library which allows to consider constitutive models written in the standard generalized thermodynamics framework as well as user-defined constitutive models. It is developed at the Department of Aerospace, Mechanics and Materials by Stainier et al. (2003).

The main idea is to include cohesive surfaces along all finite element boundaries (Xu and Needleman, 1994). So, a multibody strategy is chosen, each finite element being a body (see Figure 2).

The software allows three dimensional finite deformation simulations in heterogeneous materials from crack initiation (without initiation criteria) to post-fracture behavior.

## 5 APPLICATIONS

### 5.1 Dynamic crack propagation in a representative volume element (RVE) of hydrided Zircaloy-4

Zircaloy cladding tubes at high burn-up are considered as a bimaterial which is formed by hydride inclusions (hydride content varies gradually in the tube thickness) surrounded by a metallic matrix.

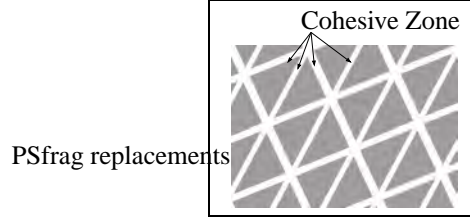


Figure 2: *Multibody strategy : each finite element is a body*

This example deals with the influence of hydride inclusions on the fracture of Zircaloy-4 during a reactivity initiated accident.

Two cases are considered : a RVE of Zircaloy-4 without hydrides and a RVE of Zircaloy-4 with hydrides distributed randomly (with a volume fraction of 30 %  $\sim$  5473 ppm) and oriented horizontally. The RVE is a square (length of a side = 10  $\mu$ m). Matrix is assumed to be elastoplastic ( $J_2$  plasticity) and hydrides neo-Hookean. The bonding strength value between the two phases is considered as “strong” ( $w^i/w^h \simeq 1$ ,  $w^i$  and  $w^h$  denote the surface energy of interface matrix/hydride and matrix/matrix respectively). The material properties and the cohesive coefficients are given in Table 1 and 2. We assume there is low friction  $\mu = 0.05$ , no post-fracture pressure  $p = 0$  and same compliance for the normal and tangential behaviors  $C_N = C_T$ . We impose velocity boundary conditions along horizontal faces :  $V = 2$  m/s (right) and  $V = -2$  m/s (left).

	Young Modulus (GPa)	Poisson's ratio	Yield in tension (MPa)	Hardening Modulus (MPa)
Matrix	98	0.325	500	1000
$\delta$ -hydride	135	0.32	-	-

Table 1: *Material properties used in the finite element calculations. The material properties correspond to irradiated Zircaloy-4 matrix and  $\delta$ -hydride.*

	$C_N = C_T$ (Pa/m)	$w$ (J/m <sup>2</sup> )
Matrix/Matrix	$10^{19}$	1
Matrix/Hydride	$2 \times 10^{19}$	1
Hydride/Hydride	$2 \times 10^{19}$	1

Table 2: *Constitutive parameters for cohesive surfaces.*

On the “strength vs imposed displacement” curve (in the left in Figure 3), the volume behavior (elastoplasticity) associated with the FCZM (surfacic behavior described by a softening function) lead to a damage elastoplasticity behavior for the Zircaloy-4.

Figure 3 shows the weakening effect of the hydrides. The introduction of 30 % volume fraction of hydrides reduces the total elongation (TE) by a factor of 5 (TE for Zircaloy-4  $\simeq$  24 %, TE for hydrided Zircaloy-4  $\simeq$  4.8 %). In this case, the behavior of the hydrided Zircaloy-4 is brittle. These results are consistent with experimental results.

Hydrides have a weakening effect : the energy release for hydrided Zircaloy-4 is approximately 80 % lower than for the non hydrided material.

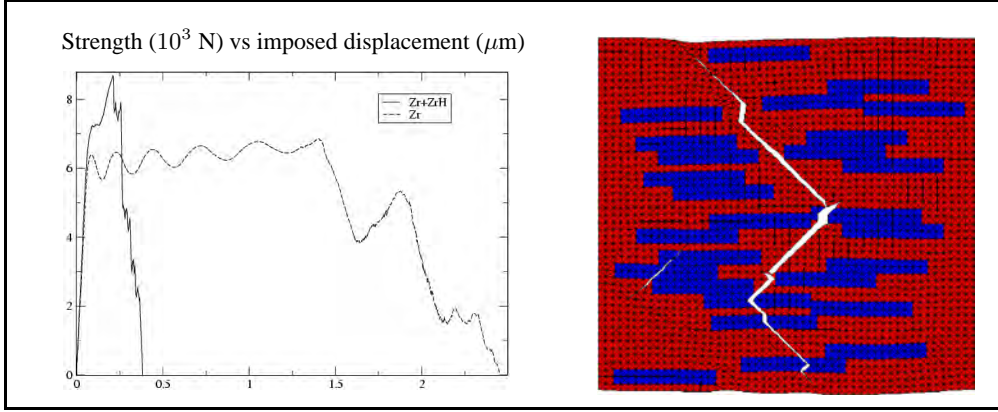


Figure 3: *Strength vs imposed displacement for Zircaloy-4 and hydrided Zircaloy-4 (5473 ppm) and rupture features of a RVE of hydrided Zircaloy-4.*

## 5.2 Macroscopic behavior of RVE of hydrided Zircaloy-4 depending on hydrogen content

This study deals with the macroscopic description of damage in hydrided Zircaloy-4 with various hydrogen contents. For that, we consider RVEs with different microstructures. Each microstructure is composed of a metallic matrix (Zircaloy-4) with rectangular elastic inclusions (hydrides) at a given volume fraction. RVEs are sufficiently large to ascertain statistical uniformity of distributed hydrides (square : length of a side = 10  $\mu\text{m}$ ).

As the example 5.1, the matrix is assumed to be elastoplastic ( $J_2$  plasticity), hydrides neo-Hookean and the bonding strength value between the two phases “strong”. The material properties and cohesive coefficients respectively are given in Table 1 and 2. We assume there is low friction  $\mu = 0.05$ , no post-fracture pressure  $p = 0$  and same compliance for the normal and tangential behaviors  $C_N = C_T$ . We impose velocity boundary conditions along horizontal faces :  $V = 2$  m/s (right) and  $V = -2$  m/s (left).

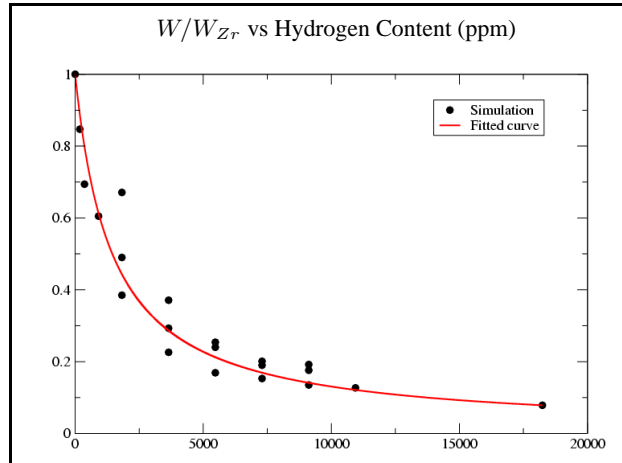


Figure 4: *Influence of hydrogen content on energy release rate.*

Figure 4 shows the energy release rate versus hydrogen content. The energy release rate decreases rapidly with hydrogen content (180 ppm of hydrogen reduces the energy release rate by 20 %, 920ppm by 40 %, 7296 ppm by 80 %). These results show the importance of the hydride and, in particular, their deleterious influence on the material ductility.

In Figure 4, the weakening effect is accurately represented by Eq. 10.

$$\frac{W}{W_{Zr}} = \frac{1 + \frac{W_i}{W_{Zr}} f}{1 + \left( \frac{W_i}{W_{Zr}} \right)^{-1} f} \quad (10)$$

where  $W$ ,  $W_{Zr}$  and  $W_i$  respectively are the macroscopical energy release rate in hydrided Zircaloy-4, Zircaloy-4 and hydrides ( $J$ ),  $f = \frac{91}{1.66 \times 10^6} [H]$  is the hydride volume fraction (%) and  $[H]$  is the hydrogen content (ppm).

## 6 CONCLUSION

This paper has presented a numerical framework for the simulation of the dynamic fracture of heterogeneous materials like hydrided Zircaloy-4. This approach is based on the coupling between the Cohesive Zone Model concept and the Non-Smooth Contact Dynamics method. The associated software is developed by coupling libraries with the Object Oriented method. The ability of this software has been illustrated on the dynamic crack propagation of hydrided Zircaloy-4. A damage elastoplastic behavior has been simulated for the Zircaloy-4 and the weakening effect of the hydrides has been emphasised. A study for the macroscopic behavior of hydrided Zircaloy-4 versus hydrogen content has been leaded.

## References

- Alart, P. and Curnier, A. (1988). *Journal de Mécanique Théorique et Appliquée*, 7:67–82.
- Dubois, F. and Jean, M. (2003). In *Actes du sixième colloque national en calcul de structures - CSMA-AFM-LMS*, volume 1, pages 111–118, Giens.
- Fremond, M. (1987). *Journal de Mécanique Théorique et Appliquée*, 6(3):383–407.
- Jean, M. (1999). *Computer Methods in Applied Mechanics and Engineering*, 177:235–257.
- Jean, M., Acary, V., and Monerie, Y. (2001). *Phil. Trans. R. Soc. Lond.*, A359:2497–2518.
- Michel, J.-C., Suquet, P., and Thébaud, F. (1994). *Revue Européenne des Elements Finis*, 3.
- Monerie, Y. and Acary, V. (2001). *Revue Européenne des Elements Finis*, 10:489–503.
- Moreau, J.-J. (1988). In Moreau, J.-J. and Panagiotopoulos, P., editors, *Non Smooth Mechanics and Applications*, volume 302 of *CISM - Courses and Lectures*, pages 1–82, Vienna. Springer.
- Piar, B., Chailan, L., and Vola, D. (2003). In *Trend in Physical and Numerical of Multiphase Industrial Flows. Cargèse*.
- Raous, M., Cangémi, L., and Cocu, M. (1999). *Computer Methods in Applied Mechanics and Engineering*, 177(3–4):383–399.
- Raous, M. and Monerie, Y. (2002). In Martins, J. and M.D.P. M. M., editors, *3d Contact Mechanics International Symposium*, Collection Solid Mechanics and its Applications, pages 333–346. Kluwer, Peniche (Portugal).
- Stainier, L., Dubois, F., and Peyroux, R. (2003). In *6ème Colloque National en Calcul des Structures*.
- Xu, X.-P. and Needleman, A. (1994). *Journal of Mechanics and Physics of Solids*, 42(9):1397–1434.